THE JOURNAL OF PHYSICAL CHEMISTRY B

Article

pubs.acs.org/JPCB

Nature of the Surface-Exposed Cytochrome−Electrode Interactions in Electroactive Biofilms of *Desulfuromonas acetoxidans*

A. Alves,[†] H. K. Ly,[‡] P. Hildebrandt,[‡] R. O. Louro,[†] and D. Millo*[,§]

[†]Instituto de Tecnologia Química e Biológica António Xavier, Universidade Nova de Lisboa, Avenida da República—Estação Agronómica Nacional, 2780-157 Oeiras, Portugal

[‡]Institut für Chemie, Technische Universität Berlin, Straße des 17. Juni 135, D-10623 Berlin, Germany

[§]Department of Physics and Astronomy, VU University Amsterdam, De Boelelaan 1081, 1081 HV Amsterdam, The Netherlands

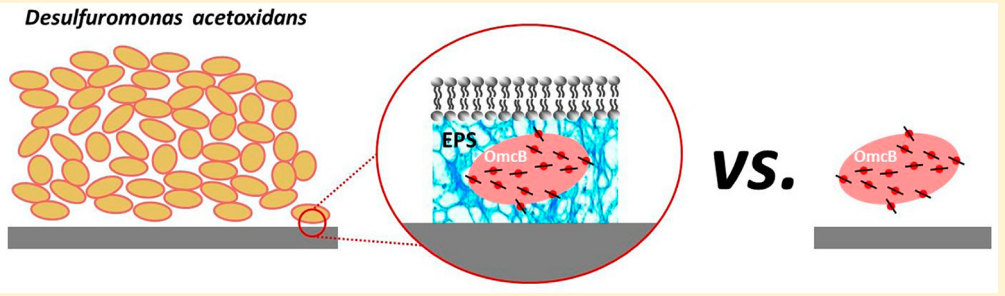

ABSTRACT: Metal-respiring bacteria are microorganisms capable of oxidizing organic pollutants present in wastewater and transferring the liberated electrons to an electrode. This ability has led to their application as catalysts in bioelectrochemical systems (BESs), a sustainable technology coupling bioremediation to electricity production. Crucial for the functioning of these BESs is a complex protein architecture consisting of several surface-exposed multiheme proteins, called outer membrane cytochromes, wiring the cell metabolism to the electrode. Although the role of these proteins has been increasingly understood, little is known about the protein−electrode interactions and their impact on the performance of BESs. In this study, we used surface-enhanced resonance Raman spectroscopy in combination with electrochemical techniques to unravel the nature of the protein−electrode interaction for the outer membrane cytochrome OmcB from *Desulfuromonas acetoxidans* (*Dace*). Comparing the spectroelectrochemical properties of OmcB bound directly to the electrode surface with those of the same protein embedded inside an electroactive biofilm, we have shown that the surface-exposed cytochromes of *Dace* biofilms are in direct contact with the electrode surface. Even if direct binding causes protein denaturation, the biofilm possesses the ability to minimize the extent of the damage maximizing the amount of cells in direct electrical communication with the electrode.

INTRODUCTION

Anaerobic microorganisms isolated from sediments and stratified bodies of water have revealed a remarkably versatile bioenergetic metabolism, often associated with transfer of electrons to the outside of the cell, a process known as extracellular electron transfer (EET).[1] These organisms gained notoriety when their vast potential for bioremediation of contaminated sediments, soils, and groundwater was discovered.[2,3] Also, their ability to transfer electrons to extracellular solid acceptors has been applied in the development of bioelectrochemical technologies,[4] which employ electrodes as final electron acceptors to harvest electricity from the bacterial metabolism.[5] The liberated electrons can be used to generate electrical energy in a microbial fuel cell or drive the bioelectrosynthesis of high value compounds such as hydrogen and methane by microorganisms attached at the cathode of a microbial electrolysis cell.[6] Research on the development of these technologies is still growing, in particular on the key aspect of the optimization of the electrical contact between the microbial metabolism and the extracellular electrodes.[7]

The molecular mechanisms for EET can be divided into direct and indirect electron transfer.[8] In direct electron transfer (DET) there is contact with the extracellular solid which can be established by redox protein complexes present at the external face of the outer membrane of the cells. Several of these complexes contain outer membrane cytochromes (OMCs) and have been found in organisms capable of performing EET.[9] DET can also occur by electrically conductive appendages, called pili or nanowires.[10,11] The direct contact between bacteria and the solid substrate is not always required.[12] Indirect or mediated electron transfer (MET) has been proposed to take place via soluble redox mediators shuttling electrons between the electrode and the OMCs. This type of electron transfer seems to be important for cells in thick biofilms which are not directly attached to the electrode surface.[8,13]

Received: April 9, 2015
Revised: May 15, 2015

DOI: 10.1021/acs.jpcb.5b03419
J. Phys. Chem. B XXXX, XXX, XXX−XXX

In view of the biotechnological interest in this subject, two bacterial species gathered most of the attention and have become model organisms in the study of EET: *Shewanella (S.) oneidensis* MR-1 and *Geobacter (G.) sulfurreducens*.[14,15] Although *S. oneidensis* MR-1 possesses a highly versatile metabolism, it uses a restricted range of carbon sources that are not completely oxidized but transformed to acetate.[2] This is in contrast to the complete oxidation of carbon sources performed by bacteria from the genera *Geobacter* and *Desulfuromonas*.[3] Studies performed with microbial fuel cells using freshwater and marine sediments showed that species from the Geobacteraceae family, such as *G. sulfurreducens* and *Desulfuromonas acetoxidans*, are the predominant species during electricity production.[16,17] Unlike *G. sulfurreducens* and *S. oneidensis*, *D. acetoxidans* is a marine organism with a higher salt tolerance.[18] In the context of operation of microbial electrochemical technologies, a marine or salt tolerant organism such as *D. acetoxidans* is advantageous, because the internal resistance of the device is lower in the presence of higher salt concentrations.

D. acetoxidans DSM 684 (*Dace*) is a δ-proteobacterium isolated from sediments of the Antarctic Ocean.[19] The draft genome of *Dace* reports 47 putative multiheme cytochromes, most of which are still unstudied. Recently, a 13 heme cytochrome from the outer membrane of this bacterium, Dace_0364 (OmcB), was purified[20] and sequence analysis showed homology with the dodecaheme OmcB cytochrome from *G. sulfurreducens*, which seems to be involved in metal respiration.[21]

This work aims to unravel the nature of the biofilm−electrode interaction for electroactive biofilms of *Dace* grown on electrodes by monitoring the spectroelectrochemical properties of the surface-exposed cytochromes wiring the cell metabolism to the electrode. Comparing the spectroelectrochemical properties of the surface-exposed cytochromes embedded inside the biofilm with those obtained for the isolated protein OmcB and the *Dace* pellets allows identification of the factors that may influence the heterogeneous ET process across the biofilm−electrode interface. The experimental approach consists of a combination of various electrochemical techniques and surface-enhanced resonance Raman (SERR) scattering. The former provide information on the redox properties of the electroactive species, while the latter monitors the structural changes of proteins promoting the electron transfer at the biofilm−electrode interface. In SERR scattering, surface-enhanced Raman (SER) and resonance Raman (RR) effects are combined. SER is responsible for the enormous enhancement of the Raman scattering that is accomplished if a protein is adjacent to a nanoscopically rough Ag surface; RR applies when the frequency of the incident light is close to an electronic transition of a chromophore (e.g., the heme group of a cytochrome) embedded in the protein. Thus, SERR spectroscopy almost exclusively probes the chromophore, since the nonresonant contributions of the protein backbone are very weak. Moreover, due to the distance-dependent attenuation of the surface enhancement effect, SERR spectroscopy selectively probes the surface-confined molecules.[22] This approach has been applied successfully to heme proteins adsorbed on Ag electrodes in the picomolar concentration range, and recently also to electroactive microbial biofilms.[23−25] A SERR spectrum of a heme protein provides structural information about the oxidation, coordination, and spin states of the central Fe atom, revealing also the nature of the axial ligands. Since the Ag support acts both as an amplifier of the incident radiation and as an electrode, performing SERR spectroscopy in combination with electrochemical techniques is a very powerful strategy to probe structural changes accompanying the heterogeneous electron transfer process promoted by heme proteins.[26]

MATERIALS AND METHODS

Bacterial Growth. *Desulfuromonas acetoxidans* DSM 684 (*Dace*) was purchased from DSMZ culture collection and cultivated as previously described.[20] The bacteria were grown using a modified basal medium containing 1.0 g of KH_2PO_4, 0.3 g of NH_4Cl, 1.0 g of $MgSO_4{\cdot}7H_2O$, 2.0 g of $MgCl_2{\cdot}6H_2O$, 20 g of NaCl, 0.1 g of $CaCl_2$, 1.77 g of Na_2SO_4, and 10 mL of Trace Element Solution SL-4 per liter as described in the catalogue of strains of the DSMZ: *Desulfuromonas acetoxidans* DSM 684 medium, 2004 (available at http://www.dsmz.de/microorganisms/medium/pdf/DSMZ_Medium95.pdf). The Trace Element Solution contained 0.5 g of EDTA, 0.2 g of $FeSO_4{\cdot}7H_2O$, 0.01 g of $ZnSO_4{\cdot}H_2O$, 0.003 g of $MnCl_2{\cdot}4H_2O$, 0.03 g of H_3BO_3, 0.02 g of $CoCl_2{\cdot}6H_2O$, 0.001 g of $CuCl_2{\cdot}H_2O$, 0.002 g of $NiCl_2{\cdot}6H_2O$, and 0.003 g of $Na_2MoO_4{\cdot}2H_2O$, per liter. Prior to inoculation, the following sterile and anoxic solutions were added to the medium: 4.0 g of $NaHCO_3$, 0.3 g of $Na_2S{\cdot}9H_2O$, and 20 μg of biotin. Sodium acetate, 15 mM, was used as carbon and electron source, and for inoculum preparation the electron acceptor was 30 mM disodium fumarate. All cultures were anaerobically grown at 30 °C, pH 7.2, and with 20% inocula. For biofilm growth on electrodes, disodium fumarate was replaced by a Ag electrode at a constant applied potential (see below), and $Na_2S{\cdot}9H_2O$ was omitted, since it reacts with the Ag tips of the electrodes. A late exponential phase *Dace* inoculum was centrifuged at 3500*g* for 20 min at room temperature. The pellet was then resuspended on basal medium containing biotin, $NaHCO_3$, and 15 mM sodium acetate at a proportion of 1:100 the original volume.

OmcB Purification. Dace_0364 (OmcB) was purified as previously described by Alves et al.,[20] using elemental sulfur as terminal electron acceptor. The concentration used for experiments was approximately 2.9 μM in 5 mM Tris buffer, pH 7.6.

Electrochemical Measurements. Measurements were done on SMARTIP electrodes (mechanical workshop of the VU University Amsterdam) equipped with a removable Ag disk, and embedded inside the homemade spectroelectrochemical cell described elsewhere.[27] Ag disks were polished with water on aluminum oxide lapping film sheets (3MTH) from 5 to 1 μm grain size until a mirrorlike appearance of the surfaces was obtained.[28] Afterward, the electrodes were roughened ex situ with the oxidation reduction cycle procedure described elsewhere,[29] and then placed into the spectroelectrochemical cell with the disk facing up. *Dace* pellets were deposited directly onto the Ag disk and the cell was quickly sealed. This operation was conducted inside a homemade box constantly purged with N_2 to reduce the exposure of the *Dace* pellets to O_2. During biofilm growth, the sealed spectroelectrochemical cell was kept inside the box at the applied potential of 0 V vs saturated calomel electrode (SCE) (Amel Instruments) and controlled by a potentiostat, PGSTAT101 (Metrohm Autolab). All potentials in this work refer to the SCE electrode.

SERR Measurements. Measurements were done on the spectroelectrochemical cell placed under a homemade Raman microscope operating in the backscattering configuration: a

DOI: 10.1021/acs.jpcb.5b03419
J. Phys. Chem. B XXXX, XXX, XXX−XXX

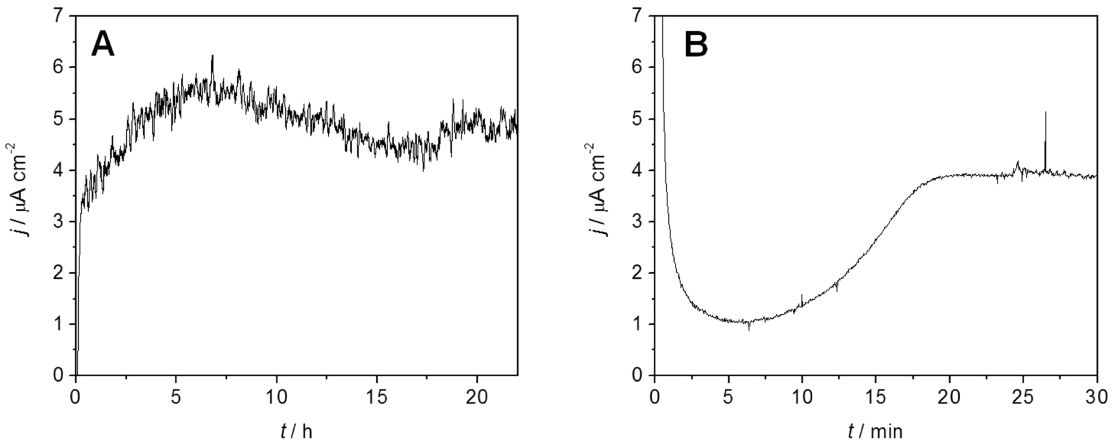

Figure 1. (A) and (B) CA traces of biofilm growth in the presence of *Dace* pellets and the recovery of electrocatalytic activity after pellet removal, respectively. The applied potential is 0 V. Note that these processes occur on different time scales.

Zeiss microscope (D-7082 with a 16× objective, numerical aperture 0.35, working distance 2 mm) coupled to an Andor Shamrock SR-303i-A single monochromator (Andor Technologies DV-420OE) with a 2400 g mm^{-1} holographic grating and an Andor Newton A-DU970N-UVB CCD camera. The 413.1 nm line of a continuous wave Kr ion laser (Innova 300C, Coherent) was used for excitation. The Rayleigh scattered light was removed using a holographic notch filter (Kaiser Optical Systems). To avoid sample photodegradation, the cell was clamped on a movable stage which ensured a rapid and constant linear movement of the cell under the microscope objective. The monochromator slit was set to 120 lines/mm, yielding a resolution of approximately 4 cm^{-1}, with an increment of approximately 0.8 cm^{-1} per data point. RR measurements on the *Dace* pellets and the isolated OmcB were done using the same setup as for SERR spectroscopy, but with the sample placed inside a 1-mm-diameter glass capillary mounted onto a homemade rotating capillary.

RESULTS AND DISCUSSION

Dace biofilms were electrochemically grown on the rough Ag electrode as follows. *Dace* pellets were deposited directly on the bare Ag electrode embedded inside a spectroelectrochemical cell and subjected to a potential of 0 V vs SCE in the absence of O_2 and in the presence of the metabolic substrate acetate. Biofilm growth was monitored by chronoamperometry (CA). Current production started immediately after inoculation and reached a plateau at 5.3 ± 1.4 $\mu A\ cm^{-2}$ (see Figure 1A), which is comparable to current densities obtained for *S. oneidensis* MR-1 and *S. puterfaciens* biofilms.[30−33] After the removal of *Dace* pellets, the spectroelectrochemical cell was washed three times and filled with fresh growth medium containing acetate. As shown in Figure 1B, this operation caused an initial loss of current production followed by a fast recovery up to the value observed in the presence of *Dace* pellets. Current generation in the absence of *Dace* pellets confirms the formation of a biofilm on the electrode, even if it is not observable by visual inspection.

CA measurements in the presence of acetate (i.e., under turnover conditions) and in the absence of *Dace* pellets were stopped at maximum current production to perform cyclic voltammetric (CV) measurements. These CV signals presented the typical sigmoid shape expected for an oxidative electrocatalytic processes (see Figure 2A). The first derivative of the

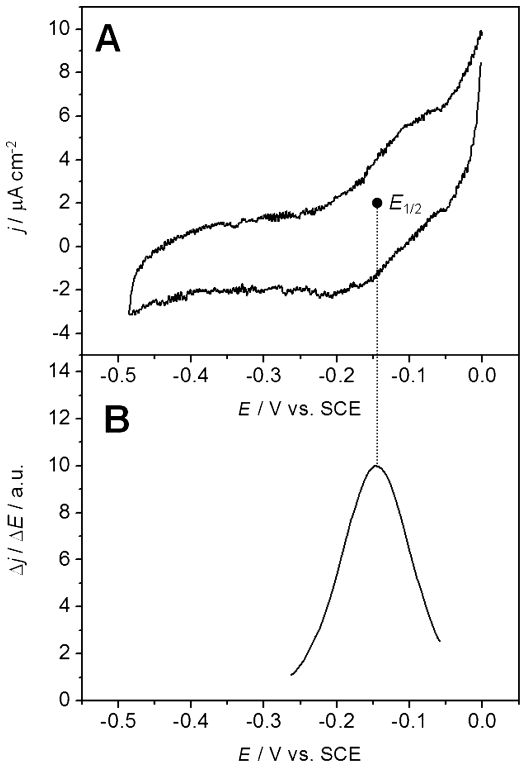

Figure 2. (A) Turnover CV trace of the *Dace* biofilm in the absence of *Dace* pellets. The CV trace is the average of three consecutive CV traces recorded on the spectroelectrochemical cell placed inside the N_2 box at the scan rate of 1 mV s^{-1}. A sigmoid curve was fitted to the ascending CV trace between −0.05 and −0.25 V. The first derivative is shown in (B).

inflection point of the CV trace under turnover conditions gave the midpoint potential ($E_{1/2}$) of the redox species promoting the heterogeneous ET.[34,35] The $E_{1/2}$ obtained with this method was −(138 ± 13) mV vs SCE, which is 215 mV more positive than that obtained for mixed culture biofilms grown on the same Ag electrode,[24] and similar to the $E_{1/2}$ observed for *S. putrefaciens* and *S. oneidensis* on different electrode materials.[30−33]

SERR spectra obtained for *Dace* biofilms in the presence of the metabolic substrate acetate were found to be potential dependent. The spectra clearly showed variations of the redox

DOI: 10.1021/acs.jpcb.5b03419
J. Phys. Chem. B XXXX, XXX, XXX−XXX

state of the heme groups with the poised potential (Figure 3A). Spectral analysis indicated the presence of at least two redox

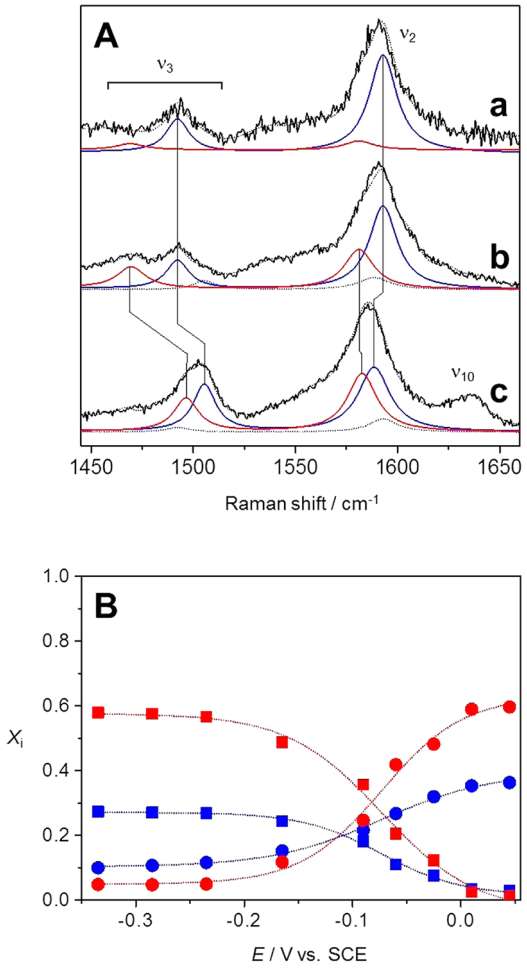

Figure 3. (A) RR spectra of *Dace* pellets in solution (a); SERR spectra of *Dace* biofilms poised at −335 (b) and +45 (c) mV vs SCE. Spectral contributions of the 6cLS and the 5cHS species are depicted in blue and red, respectively. Dotted colored lines denote minor spectral components. Dotted black lines represent the fit of the component spectra to the experimental spectra. Spectra were normalized with respect to the intensity of the ν_3 band. To avoid overcrowding, we have shown only the spectral components discussed in the text. (B) Circles and squares represent the molar fraction X_i of the oxidized and the reduced heme, respectively. 6cLS and 5cHS species are depicted in blue and red, respectively. Dotted lines show the Nernstian fit to the respective data sets.

species in two different oxidation states (see Table 1 for the band assignment): a six-coordinated low spin (6cLS) species consistent with a His-Fe-His axial ligation (bis-His), and a prevailing five-coordinated high spin (5cHS) species (see below). Since the 6cLS species was dominant in RR experiments on *Dace* pellets before inoculation (see Figure 3A), the non-native 5cHS contribution observed in the SERR spectra is the specific consequence of the biofilm−electrode interaction. Since such non-native (5cHS) heme species are often observed when a heme protein interacts directly with a bare Ag surface,[36,37] we conclude that the surface-exposed cytochromes at the biofilm−electrode interface are in direct contact with the Ag electrode. This finding differs from what we previously observed for mixed culture biofilms grown on rough Ag electrodes.[25] This discrepancy may arise from differences in the chemical composition of the bacterial cells interacting with the Ag surface, probably due to the different dominant microorganism, or may reflect the different growth procedure adopted in these cases. In fact, while in the cited paper the diluted inoculum was placed in a cell and the solution was constantly stirred, in this work the concentrated *Dace* pellets were placed directly on the Ag electrode embedded inside a spectroelectrochemical cell. This configuration of the spectroelectrochemical cell operating as described in ref 27, and the lack of stirring, allowed for the fast and immediate deposition of *Dace* cells onto the electrode, thus promoting a faster interaction between the surface-exposed cytochromes and the bare Ag surface.

SERR spectra obtained during the redox titration of the OMCs at the biofilm−electrode interface were analyzed according to the procedure described elsewhere using the spectral components of four heme species (i.e., the 6cLS and the 5cHS species in two oxidation states).[38−42] As shown in Figure 2B, the molar fractions X_i of the oxidized and the reduced species varied according to the applied potential. The Nernstian analysis of the data sets in Figure 3B gave $E_{1/2} = -(142 \pm 75)$ and $-(135 \pm 78)$ mV vs SCE for the 5cHS and the 6cLS species, respectively. Both values are in agreement with the $E_{1/2}$ obtained via CV, thus indicating that the surface-exposed cytochromes detected by SERR spectroscopy are the same ones probed by CV and mediate the electron transfer at the biofilm−electrode interface. The number of electrons exchanged during the process was $0.3 \leq n \leq 0.7$ for the 6cLS and the 5cHS species. Both values are considerably smaller than 1, which is the expected value for a one-electron oxidation and/or reduction of the heme iron. Even if the low n value may be indicative of an inaccurate fitting,[26] the virtually perfect match between the $E_{1/2}$ values obtained with CV and SERR spectroscopy excludes this possibility. Indeed, we tentatively ascribe the low n value to a dispersion of $E_{1/2}$ and/or electron transfer rate constants at the biofilm−electrode interface, which results in a sigmoid-shaped curve with a reduced steepness in the middle region. As proposed by Bowden and co-workers, this may be due to the heterogeneity of the surface-exposed cytochromes in direct contact with the electrode.[43] To better understand the effect of the electrode surface on the surface-exposed cytochromes, we performed similar experiments on the

Table 1. Spectral Parameters of the Heme Species Observed in This Work[a]

Fe^{3+} heme states				Fe^{2+} heme states			
mode	6cLS His-Fe-His	6cHS His-Fe-X	5cHS His-Fe-	mode	6cLS His-Fe-His	6cHS His-Fe-X	5cHS His-Fe-
ν_4	1374	1366	1368	ν_4	1361	1345	1354
ν_3	1505	1485	1498	ν_3	1492	1467	1469
ν_2	1588	1572	1577−1582	ν_2	1593	1564	1573−1581

[a]Frequencies are given in cm^{-1}.

DOI: 10.1021/acs.jpcb.5b03419
J. Phys. Chem. B XXXX, XXX, XXX−XXX

isolated protein OmcB. This protein was purified from cells grown with elemental sulfur as terminal electron acceptor, and is also predicted to be the terminal reductase for the respiration/reduction of metals and electrodes.[20] Homology studies demonstrated that this protein is part of a trans-outer membrane porin−cytochrome protein complex common to other species of bacteria performing EET.[44] As in the case of *Dace* biofilms, RR spectra of OmcB in solution showed only the His-Fe-His heme contribution, which turned into a mixture of the native bis-His and two non-native HS species when OmcB was immobilized on roughened Ag electrodes (Figure 4A). These non-native species are the 5cHS His-Fe species and an unusual six-coordinated high spin (6cHS) conformer, probably featuring a His-Fe-X axial ligation with X = H_2O or another weakly electron-donating molecule, as inferred by the outstanding low frequency of the vibrational mode ν_4 in the reduced state (see Table 1 and Figure 4B). Such a low ν_4 frequency is observed for the electron-rich fifth ligand in combination with a weak coordinating sixth ligand for example present in the heme of cytochrome P450, i.e., thiolate and water, respectively.[40] CV experiments did not feature any voltammetric peak, probably due to the dispersion of midpoint potentials and/or electron transfer rate constants, thus making impossible the determination of $E_{1/2}$ with this technique. $E_{1/2}$ was thus obtained with the SERR redox titration described above.

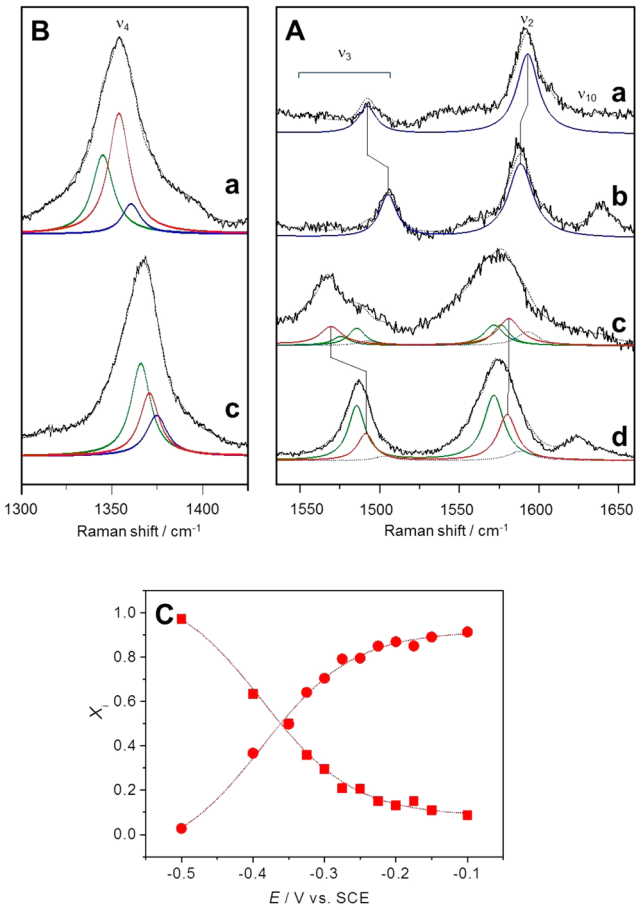

Figure 4. (A) Resonance Raman spectra of isolated OmcB in solution reduced via dithionite (a) and before adding dithionite (b). SERR spectra of isolated OmcB adsorbed on rough Ag electrode at the poised potential of −500 (c) and 0 (d) mV vs SCE. Spectral contributions of the 6cLS, the 5cHS, and the 6cHS species are depicted in blue, red, and green, respectively. Spectra were normalized with respect to the intensity of the ν_3 band. (B) ν_4 region of the SERR spectra a and c depicted in (A). Spectra in (B) were normalized with respect to the intensity of the ν_4 band. The dotted colored lines denote minor spectral components. Dotted black lines represent the fit. For the sake of simplicity, we have shown only the spectral components discussed in the text. (C) Circles and squares represent the molar fraction X_i of the oxidized and the reduced 5cHS heme species, respectively. Dotted lines show the Nernstian fit of the data sets.

SERR spectra obtained at different poised potentials were simulated by fitting six spectral components to the data, accounting for the 6cLS, the 5cHS, and the 6cHS species in both oxidation states. As shown in Figure 4A, the contribution of the redox-active 6cLS species to the SERR spectra is very minor. On the other hand, the 6cHS species is largely redox inactive, as shown by the presence of oxidized 6cHS contributions at negative applied potentials. Accordingly, the main species undergoing oxidation and reduction is the 5cHS species. The Nernst analysis of the data in Figure 4C afforded $E_{1/2} = -(383 \pm 4)$ mV, which is ca. 250 mV more negative than that of the surface-exposed cytochromes embedded in living biofilms grown on the same electrode. As for *Dace* biofilms, the n value ranging from 0.4 to 0.8 may be explained by a dispersion of midpoint potentials and/or electron transfer rate constants caused by the OmcB−Ag interaction (see above). Thus, our results show that the structural and redox properties of the isolated OmcB differ from those of the surface-exposed cytochromes embedded in a living *Dace* biofilm significantly. This leads to two possible scenarios. Even if OmcB is involved in the EET, it does not promote the heterogeneous ET across the biofilm−electrode interface. Alternatively, OmcB does indeed contribute to the heterogeneous ET. The differences between the isolated OmcB and the *Dace* biofilm may be tentatively explained considering the ability of *Dace* cells to control protein orientation accurately and use extracellular polysaccharide substances (EPS) to buffer protein−electrode interactions. In fact, while the isolated OmcB can interact with the Ag surface through the whole protein surface, the spatial constraints of the OmcB bound to the outer membrane of *Dace* cells—probably directly attached to a porin−cytochrome protein complex—limit the exposure to the electrode of a much smaller fraction of protein surface. Accordingly, the extent of protein denaturation is different for OmcB when it binds directly to the Ag surface as an isolated protein or when it interacts with the metallic support as a part of the cellular system. This observation suggests that EPS on *Dace* cell surface reduce the amount of damage deriving from direct protein−electrode interactions. Even if the way microbes control protein−electrode interactions is presently unknown, our data suggest that the underlying strategy aims to minimize the amount of redox-inactive species on the electrode to ensure the survival of the maximum number of cells. This may be a general strategy for metal-respiring bacteria, since also the surface-exposed cytochromes of *S. oneidensis* MR-1 seem to maintain the native conformation upon direct binding with Ag nanoparticles on the microorganism.[45]

CONCLUSIONS

We grew electroactive biofilms of *Dace* on rough Ag electrodes obtaining current densities and $E_{1/2}$ similar to those observed for *Shewanella* species. Spectroelectrochemical analyses of the biofilm and its isolated components (i.e., *Dace* cells before inoculation and the isolated OmcB in solution and on the

DOI: 10.1021/acs.jpcb.5b03419
J. Phys. Chem. B XXXX, XXX, XXX−XXX

electrode) showed that the surface-exposed cytochromes promoting the ET at the biofilm−electrode interface are in direct contact with the Ag electrode. Substantial differences between the spectroelectrochemical properties of the isolated OmcB and the surface-exposed cytochromes embedded inside the *Dace* biofilm suggest that either this protein does not promote the interfacial ET or other factors control the protein−electrode interactions lowering the risks of protein denaturation to reduce the presence of electrochemically inactive species on the electrode.

AUTHOR INFORMATION

Corresponding Author

*E-mail: d.millo@vu.nl.

Author Contributions

A.A. and H.K.L. contributed equally to this work

Notes

The authors declare no competing financial interest.

ACKNOWLEDGMENTS

The work was supported by The Netherlands Organisation for Scientific Research. D.M. and A.A. acknowledge the Caesar Foundation for a generous grant and the LaserLaB Access Program (Project No. LLAMS001985, LASERLAB-EUROPE Grant Agreement No. 284464, EC's Seventh Framework Programme). P.H. acknowledges the support by UniCat, funded by the Deutsche Forschungsgemeinschaft.

REFERENCES

(1) Hau, H. H.; Gralnick, J. A. Ecology and Biotechnology of the Genus Shewanella. *Annu. Rev. Microbiol.* **2007**, *61*, 237−258.

(2) Nealson, K. H.; Belz, A.; McKee, B. Breathing Metals as a Way of Life: Geobiology in Action. *Antonie van Leeuwenhoek* **2002**, *81*, 215−222.

(3) Lovley, D. R. Bioremediation. Anaerobes to the Rescue. *Science* **2001**, *293*, 1444−1446.

(4) Logan, B. E.; Rabaey, K. Conversion of Wastes into Bioelectricity and Chemicals by Using Microbial Electrochemical Technologies. *Science* **2012**, *337*, 686−690.

(5) Logan, B. E. Scaling up Microbial Fuel Cells and Other Bioelectrochemical Systems. *Appl. Microbiol. Biotechnol.* **2010**, *85*, 1665−1671.

(6) Marshall, C. W.; Ross, D. E.; Fichot, E. B.; Norman, R. S.; May, H. D. Long-Term Operation of Microbial Electrosynthesis Systems Improves Acetate Production by Autotrophic Microbiomes. *Environ. Sci. Technol.* **2013**, *47*, 6023−6029.

(7) Rosenbaum, M. A.; Henrich, A. W. Engineering Microbial Electrocatalysis for Chemical and Fuel Production. *Curr. Opin. Biotechnol.* **2014**, *29*, 93−98.

(8) Gralnick, J. A.; Newman, D. K. Extracellular Respiration. *Mol. Microbiol.* **2007**, *65*, 1−11.

(9) Richardson, D. J.; Butt, J. N.; Fredrickson, J. K.; Zachara, J. M.; Shi, L.; Edwards, M. J.; White, G.; Baiden, N.; Gates, A. J.; Marritt, S. J.; et al. The "Porin-Cytochrome" Model for Microbe-to-Mineral Electron Transfer. *Mol. Microbiol.* **2012**, *85*, 201−212.

(10) Gorby, Y. A.; Yanina, S.; McLean, J. S.; Rosso, K. M.; Moyles, D.; Dohnalkova, A.; Beveridge, T. J.; Chang, I. S.; Kim, B. H.; Kim, K. S.; et al. Electrically Conductive Bacterial Nanowires Produced by Shewanella Oneidensis Strain MR-1 and Other Microorganisms. *Proc. Natl. Acad. Sci. U. S. A.* **2006**, *103*, 11358−11363.

(11) Reguera, G.; McCarthy, K. D.; Mehta, T.; Nicoll, J. S.; Tuominen, M. T.; Lovley, D. R. Extracellular Electron Transfer via Microbial Nanowires. *Nature* **2005**, *435*, 1098−1101.

(12) Newman, D. K.; Kolter, R. A Role for Excreted Quinones in Extracellular Electron Transfer. *Nature* **2000**, *405*, 94−97.

(13) Paquete, C. M.; Fonseca, B. M.; Cruz, D. R.; Pereira, T. M.; Pacheco, I.; Soares, C. M.; Louro, R. O. Exploring the Molecular Mechanisms of Electron Shuttling across the Microbe/metal Space. *Front. Microbiol.* **2014**, *5*, 1−12.

(14) Myers, C. R.; Nealson, K. H. Bacterial Manganese Reduction and Growth with Manganese Oxide as the Sole Electron Acceptor. *Science* **1988**, *240*, 1319−1321.

(15) Lovley, D. R.; Phillips, E. J. Novel Mode of Microbial Energy Metabolism: Organic Carbon Oxidation Coupled to Dissimilatory Reduction of Iron or Manganese. *Appl. Environ. Microbiol.* **1988**, *54*, 1472−1480.

(16) Lovley, D. R. Bug Juice: Harvesting Electricity with Microorganisms. *Nat. Rev. Microbiol.* **2006**, *4*, 497−508.

(17) Lovley, D. R. Extracellular Electron Transfer: Wires, Capacitors, Iron Lungs, and More. *Geobiology* **2008**, *6*, 225−231.

(18) Widdle, F.; Pfennig, N. In *The Prokaryotes: A Handbook on the Biology of Bacteria: Ecophysiology, Isolation, Identification, Applications Vol. IV*; Balows, A., Triipe, G. H., Dworkin, M., Harder, W., Schleifer, K. H., Eds.; Springer Science: New York, 1992; pp 3379−3389.

(19) Pfennig, N.; Biebl, H. Desulfuromonas Acetoxidans Gen. Nov. and Sp. Nov., A New Anaerobic, Sulfur-Reducing, Acetate-Oxidizing Bacterium. *Arch. Microbiol.* **1976**, *110*, 3−12.

(20) Alves, A. S.; Paquete, C. M.; Fonseca, B. M.; Louro, R. O. Exploration of the "Cytochromome" of Desulfuromonas Acetoxidans, a Marine Bacterium Capable of Powering Microbial Fuel Cells. *Metallomics* **2011**, *3*, 349−353.

(21) Butler, J. E.; Young, N. D.; Lovley, D. R. Evolution of Electron Transfer out of the Cell: Comparative Genomics of Six Geobacter Genomes. *BMC Genomics* **2010**, *11*, No. 40, DOI: 10.1186/1471-2164-11-40.

(22) Siebert, F.; Hildebrandt, P. *Vibrational Spectroscopy in Life Science*; Wiley-VCH: Weinheim, Germany, 2008.

(23) Sezer, M.; Millo, D.; Weidinger, I. M.; Zebger, I.; Hildebrandt, P. Analyzing the Catalytic Processes of Immobilized Redox Enzymes by Vibrational Spectroscopies. *IUBMB Life* **2012**, *64*, 455−464.

(24) Millo, D.; Harnisch, F.; Patil, S. A.; Ly, H. K.; Schröder, U.; Hildebrandt, P. In Situ Spectroelectrochemical Investigation of Electrocatalytic Microbial Biofilms by Surface-Enhanced Resonance Raman Spectroscopy. *Angew. Chem., Int. Ed.* **2011**, *50*, 2625−2627.

(25) Ly, H. K.; Harnisch, F.; Hong, S.-F.; Schröder, U.; Hildebrandt, P.; Millo, D. Unraveling the Interfacial Electron Transfer Dynamics of Electroactive Microbial Biofilms Using Surface-Enhanced Raman Spectroscopy. *ChemSusChem* **2013**, *6*, 487−492.

(26) Millo, D. Spectroelectrochemical Analyses of Electroactive Microbial Biofilms. *Biochem. Soc. Trans.* **2012**, *40*, 1284−1290.

(27) Bonifacio, A.; Millo, D.; Gooijer, C.; Bosgschoten, R.; Van Der Zwan, G. Linearly Moving Low-Volume Spectroelectrochemical Cell for Microliter-Scale Surface-Enhanced Resonance Raman Spectroscopy of Heme Proteins. *Anal. Chem.* **2004**, *76*, 1529−1531.

(28) Millo, D.; Ranieri, A.; Koot, W.; Gooijer, C.; Van Der Zwan, G. Towards Combined Electrochemistry and Surface-Enhanced Resonance Raman of Heme Proteins: Improvement of Diffusion Electrochemistry of Cytochrome c at Silver Electrodes Chemically Modified with 4-Mercaptopyridine. *Anal. Chem.* **2006**, *78*, 5622−5625.

(29) Millo, D.; Bonifacio, A.; Ranieri, A.; Borsari, M.; Gooijer, C.; van der Zwan, G. Voltammetric and Surface-Enhanced Resonance Raman Spectroscopic Characterization of Cytochrome C Adsorbed on a 4-Mercaptopyridine Monolayer on Silver Electrodes. *Langmuir* **2007**, *23*, 4340−4345.

(30) Babauta, J. T.; Nguyen, H. D.; Beyenal, H. Redox and pH Microenvironments within Shewanella Oneidensis MR-1 Biofilms Reveal an Electron Transfer Mechanism. *Environ. Sci. Technol.* **2011**, *45*, 6654−6660.

(31) Okamoto, A.; Nakamura, R.; Hashimoto, K. In-Vivo Identification of Direct Electron Transfer from Shewanella Oneidensis MR-1 to Electrodes via Outer-Membrane OmcA-MtrCAB Protein Complexes. *Electrochim. Acta* **2011**, *56*, 5526−5531.

(32) Rosenbaum, M.; Cotta, M. A.; Angenent, L. T. Aerated Shewanella Oneidensis in Continuously Fed Bioelectrochemical

DOI: 10.1021/acs.jpcb.5b03419
J. Phys. Chem. B XXXX, XXX, XXX−XXX

Systems for Power and Hydrogen Production. *Biotechnol. Bioeng.* **2010**, *105*, 880−888.
(33) Carmona-Martínez, A. A.; Harnisch, F.; Kuhlicke, U.; Neu, T. R.; Schröder, U. Electron Transfer and Biofilm Formation of Shewanella Putrefaciens as Function of Anode Potential. *Bioelectrochemistry* **2013**, *93*, 23−29.
(34) Heering, H. A.; Hirst, J.; Armstrong, F. A. Interpreting the Catalytic Voltammetry of Electroactive Enzymes Adsorbed on Electrodes. *J. Phys. Chem. B* **1998**, *102*, 6889−6902.
(35) Fricke, K.; Harnisch, F.; Schröder, U. On the Use of Cyclic Voltammetry for the Study of Anodic Electron Transfer in Microbial Fuel Cells. *Energy Environ. Sci.* **2008**, *1*, 144.
(36) Smulevich, G.; Spiro, T. G. Surface Enhanced Raman Spectroscopic Evidence That Adsorption on Silver Particles Can Denature Heme Proteins. *J. Phys. Chem.* **1985**, *89*, 5168−5173.
(37) Wackerbarth, H.; Hildebrandt, P. Redox and Conformational Equilibria and Dynamics of Cytochrome c at High Electric Fields. *ChemPhysChem* **2003**, *4*, 714−724.
(38) Hildebrandt, P.; Stockburger, M. Cytochrome c at Charged Interfaces. 1. Conformational and Redox Equilibria at the Electrode/electrolyte Interface Probed by Surface-Enhanced Resonance Raman Spectroscopy. *Biochemistry* **1989**, *28*, 6710−6721.
(39) Murgida, D. H.; Hildebrandt, P. Redox and Redox-Coupled Processes of Heme Proteins and Enzymes at Electrochemical Interfaces. *Phys. Chem. Chem. Phys.* **2005**, *7*, 3773−3784.
(40) Oellerich, S.; Wackerbarth, H.; Hildebrandt, P. Spectroscopic Characterization of Nonnative Conformational States of Cytochrome c. *J. Phys. Chem. B* **2002**, *106*, 6566−6580.
(41) Ly, H. K.; Utesch, T.; Díaz-Moreno, I.; García-Heredia, J. M.; De La Rosa, M. Á.; Hildebrandt, P. Perturbation of the Redox Site Structure of Cytochrome c Variants upon Tyrosine Nitration. *J. Phys. Chem. B* **2012**, *116*, 5694−5702.
(42) Ly, H. K.; Wisitruangsakul, N.; Sezer, M.; Feng, J.-J.; Kranich, A.; Weidinger, I. M.; Zebger, I.; Murgida, D. H.; Hildebrandt, P. Electric-Field Effects on the Interfacial Electron Transfer and Protein Dynamics of Cytochrome c. *J. Electroanal. Chem.* **2011**, *660*, 367−376.
(43) Clark, R. A.; Bowden, E. F. Voltammetric Peak Broadening for Cytochrome c/Alkanethiolate Monolayer Structures: Dispersion of Formal Potentials. *Langmuir* **1997**, *13*, 559−565.
(44) Liu, Y.; Wang, Z.; Liu, J.; Levar, C.; Edwards, M. J.; Babauta, J. T.; Kennedy, D. W.; Shi, Z.; Beyenal, H.; Bond, D. R.; et al. A Trans-Outer Membrane Porin-Cytochrome Protein Complex for Extracellular Electron Transfer by Geobacter Sulfurreducens PCA. *Environ. Microbiol. Rep.* **2014**, *6*, 776−785.
(45) Wang, Y.; Sevinc, P. C.; Belchik, S. M.; Fredrickson, J.; Shi, L.; Lu, H. P. Single-Cell Imaging and Spectroscopic Analyses of Cr(VI) Reduction on the Surface of Bacterial Cells. *Langmuir* **2013**, *29*, 950−956.

DOI: 10.1021/acs.jpcb.5b03419
J. Phys. Chem. B XXXX, XXX, XXX−XXX